Critical structure factors of bilinear fields in O(N) vector models

Pasquale Calabrese,[1,*] Andrea Pelissetto,[2,†] and Ettore Vicari[3,‡]
[1]*Scuola Normale Superiore and INFN, Sezione di Pisa, I-56100 Pisa, Italy*
[2]*Dipartimento di Fisica, Università di Roma La Sapienza and INFN, Sezione di Roma, I-00185 Roma, Italy*
[3]*Dipartimento di Fisica, Università di Pisa and INFN, Sezione di Pisa, I-56100 Pisa, Italy*
(Received 8 November 2001; published 2 April 2002)

We compute the two-point correlation functions of general quadratic operators in the high-temperature phase of the three-dimensional O(N) vector model by using field-theoretical methods. In particular, we study the small- and large-momentum behavior of the corresponding scaling functions, and give general interpolation formulas based on a dispersive approach. Moreover, we determine the crossover exponent ϕ_T associated with the traceless tensorial quadratic field, by computing and analyzing its six-loop perturbative expansion in fixed dimension. We find $\phi_T=1.184(12)$, $\phi_T=1.271(21)$, and $\phi_T=1.40(4)$ for $N=2,3,5$, respectively.

DOI: 10.1103/PhysRevE.65.046115 PACS number(s): 05.70.Jk, 64.60.Fr, 75.40.Cx, 61.30.−v

I. INTRODUCTION

In nature, many physical systems undergo phase transitions belonging to universality classes of the O(N) vector models. Their universal critical properties can be determined theoretically by considering the ϕ^4 Hamiltonian

$$\mathcal{H}=\int d^dx\left[\frac{1}{2}\partial_\mu\vec{\phi}\cdot\partial_\mu\vec{\phi}+\frac{1}{2}r\vec{\phi}\cdot\vec{\phi}+\frac{1}{4!}u(\vec{\phi}\cdot\vec{\phi})^2\right], \quad (1)$$

where $\vec{\phi}(x)$ is an N-component real field. Various computational methods, supported by renormalization-group (RG) theory, have provided accurate determinations of several universal quantities; see, e.g., Ref. [1] for a recent comprehensive review. Among others, we should mention the critical exponents, the equation of state, and the correlation functions of the order parameter $\vec{\phi}(x)$. However, for some experimental systems one is also interested in the behavior of correlation functions describing the critical fluctuations of secondary, quadratic local fields. Due to the symmetry of the theory, there are two independent quantities that are quadratic in the fundamental field $\vec{\phi}(x)$: one is the local energy density

$$E(x)=\vec{\phi}(x)\cdot\vec{\phi}(x), \quad (2)$$

which is O(N) invariant; the other one is the anisotropic second-order traceless tensor

$$T_{ij}(x)=\phi_i(x)\phi_j(x)-\delta_{ij}\frac{1}{N}\vec{\phi}(x)\cdot\vec{\phi}(x). \quad (3)$$

The crossover exponent ϕ_T associated with the traceless tensor field $T_{ij}(x)$ describes the instability of the O(N)-symmetric theory against anisotropy [2–5]. It is thus relevant for the description of multicritical phenomena, for instance, the critical behavior near a bicritical point where two critical lines with O(N) and O(M) symmetry meet, giving rise to a critical theory with enlarged O($N+M$) symmetry, see, e.g., Refs. [6–8]. This bicritical behavior has been the object of new studies quite recently, since it appears in the SO(5) theory of superconductivity [9], and has been observed experimentally in organic conductors [10]. As discussed in Ref. [11], the correlation functions $G_E(x-y)\equiv\langle E(x)E(y)\rangle$ and $G_T(x-y)\equiv\langle T_{ij}(x)T_{ij}(y)\rangle$ are relevant in the description of strain-strain correlations in certain liquids and solids, where an effective coupling between the order parameter and the elastic deformations occurs. Moreover, in the special case $N=2$, the traceless tensor field $T_{ij}(x)$ is related to the second-harmonic order parameter in density-wave systems, whose critical behavior belongs to the XY universality class, see, e.g., Refs. [11–13]. Experimentally, such behavior is observed at the nematic–smectic-A transition in liquid crystals [11,12,14–18]. In these systems the structure factor of the secondary order parameter T_{ij} has been measured using x-ray scattering techniques [17,18]. The crossover exponent ϕ_T is also relevant [19] in the description of crossover effects in diluted Ising antiferromagnets with n-fold degenerate ground state [20], for instance, in some diluted magnetic semiconductors such as $Cd_{1-x}Mn_xTe$.

In this paper, we determine the crossover exponent ϕ_T. Such a quantity has already been obtained in the framework of the ϵ expansion to three loops [21], from the analysis of high-temperature expansions [6] for $N=2,3$, and by means of a Monte Carlo simulation [22] for $N=5$. Here, we consider the alternative field-theoretical (FT) method based on a fixed-dimension expansion in powers of the zero-momentum quartic coupling [23], and perform a six-loop calculation of ϕ_T. For the physically interesting cases $N=2,3,5$ we obtain

$$\phi_T=1.184(12)\quad(N=2),$$

$$\phi_T=1.271(21)\quad(N=3),$$

$$\phi_T=1.40(4)\quad(N=5). \quad (4)$$

We also consider the correlation functions $G_E(x)$ and $G_T(x)$ in the high-temperature phase. In the critical limit, the

*Email address: Pasquale.Calabrese@df.unipi.it
†Email address: Andrea.Pelissetto@roma1.infn.it
‡Email address: Ettore.Vicari@df.unipi.it

Fourier transform $\widetilde{G}_T(q)$ obeys a scaling law that is analogous to that of the fundamental correlation function, i.e.,

$$\widetilde{G}_T(q,t) = A_T^+ t^{-\gamma_T} f_T(q^2\xi^2), \tag{5}$$

where $t \equiv (T-T_c)/T_c$ is the reduced temperature, $\gamma_T = 2\phi_T - 2 + \alpha$ is the tensor susceptibility exponent, and ξ is the second-moment correlation length computed from the two-point function of the order parameter. The same scaling behavior holds for the correlation functions $\widetilde{G}_E(q,t)$ of systems in the Ising universality class, with α replacing γ_T, i.e., $\widetilde{G}_E(q,t) = A_E^+ t^{-\alpha} f_E(q^2\xi^2)$. For $N \geqslant 2$, however, α is negative and an additional background term should be taken into account. In this case, in the critical limit, we have

$$\widetilde{G}_E(q,t) = B_E + \widetilde{G}_{E,\text{sing}}(q,t) = B_E + A_E^+ t^{-\alpha} f_E(q^2\xi^2). \tag{6}$$

The background term B_E is the dominant one and the singular part vanishes at criticality. In this case, by using positivity (unitarity in FT language) arguments, one may also show that $A_E^+ < 0$, as observed in experiments.

In this paper we extend the two-loop ϵ-expansion computation of Refs. [11,18]. We compute the universal scaling functions $f_E(q^2\xi^2)$ and $f_T(q^2\xi^2)$ using the ϵ expansion and the expansion in fixed dimension $d=3$. First, we determine the small-momentum behavior to four loops in the fixed-dimension expansion and to three loops in ϵ expansion. In particular, we obtain accurate estimates of the experimentally relevant ratios $X_{E,T} \equiv \xi_{E,T}^2/\xi^2$, where $\xi_{E,T}$ is the second-moment correlation length computed from $G_{E,T}(x)$ or from its singular part if α is negative. For instance, for $N=1$, we find

$$X_E = 0.0140(5), \tag{7}$$

and for $N=2$,

$$X_E = -0.0017(1), \quad X_T = 0.041(2). \tag{8}$$

(We shall later comment on the negative value of X_E.) Moreover, we study the large-momentum behavior of the structure factors and construct interpolations valid for all momenta by using the dispersive approach applied to $\langle \phi(0)\phi(x)\rangle$ by Bray [24].

The paper is organized as follows. In Sec. II we report the computation of the crossover exponent ϕ_T to six loops in the fixed-dimension expansion and compare our results with the existing theoretical and experimental estimates (Sec. II D). In Sec. III we report the computation of the structure factors. In Sec. III A we briefly summarize the expected behavior of the structure factors in the critical region and set our notations. In Sec. III B we explain our FT calculation, whose results are presented in Sec. III C. In Sec. III D we finally give approximate expressions for the structure factors by using a dispersive approach. In Sec. IV we briefly discuss some physical systems where our results can be applied and compared with experiments. Appendix A discusses the large-momentum behavior of the structure factors. Details of the perturbative calculation are reported in Appendix B.

II. THE CROSSOVER EXPONENT ASSOCIATED WITH THE TENSOR COMPOSITE FIELD

A. Zero-momentum scaling behavior

The zero-momentum behavior of correlation functions involving generic local operators $\mathcal{O}(x)$, such as $E(x)$ and $T_{ij}(x)$, can be obtained from the free energy in the presence of an external field $h_\mathcal{O}$ coupled with $\mathcal{O}(x)$. Indeed, the singular part of the free energy scales as [6]

$$F_{\text{sing}} \propto t^{2-\alpha} f(h/t^{\beta+\gamma}, h_\mathcal{O}/t^{\phi_\mathcal{O}}), \tag{9}$$

where h is the magnetic field and $\phi_\mathcal{O}$ is the crossover exponent. Then, by differentiating with respect to $h_\mathcal{O}$, one obtains the zero-momentum correlations and the RG relations

$$\beta_\mathcal{O} = 2 - \alpha - \phi_\mathcal{O},$$

$$\gamma_\mathcal{O} = -2 + \alpha + 2\phi_\mathcal{O}, \tag{10}$$

where the exponents $\beta_\mathcal{O}$ and $\gamma_\mathcal{O}$ describe, respectively, the critical (singular) behavior of the average $\langle \mathcal{O}(x)\rangle \sim |t|^{\beta_\mathcal{O}}$ and of the susceptibility $\chi_\mathcal{O} \equiv \Sigma_x \langle \mathcal{O}(0)\mathcal{O}(x)\rangle_c \sim t^{-\gamma_\mathcal{O}}$.

In this section we compute the crossover exponent ϕ_T associated with the tensor field $T_{ij}(x)$ in the fixed-dimension FT framework, by performing a six-loop perturbative expansion. Of course, the crossover exponent associated with the energy density $E(x)$ is trivial, i.e., $\phi_E = 1$ and $\gamma_E = \alpha$.

B. The fixed-dimension expansion: Generalities

In the fixed-dimension FT approach, one renormalizes the theory by introducing a set of zero-momentum conditions for the two-point and four-point one-particle irreducible correlation functions

$$\Gamma_{ij}^{(2)}(p) = \delta_{ij} Z_\phi^{-1}[m^2 + p^2 + O(p^4)], \tag{11}$$

$$\Gamma_{ijkl}^{(4)}(0) = m^\epsilon Z_\phi^{-2} g \tfrac{1}{3}(\delta_{ij}\delta_{kl} + \delta_{ik}\delta_{jl} + \delta_{il}\delta_{jk}), \tag{12}$$

where $\epsilon \equiv 4-d$ and d is the space dimension. They relate the mass m and the zero-momentum renormalized coupling g to the corresponding Hamiltonian parameters r and u as

$$u = m^\epsilon g Z_u(g) Z_\phi(g)^{-2}. \tag{13}$$

In addition, one introduces the function Z_t that is defined by the relation

$$\Gamma_{ij}^{(1,2)}(0) = \delta_{ij} Z_t(g)^{-1}, \tag{14}$$

where $\Gamma^{(1,2)}(p)$ is the one particle irreducible two-point function with an insertion of the operator $\frac{1}{2}\vec{\phi}^2$.

The critical theory is obtained by setting $g = g^*$, where g^* is the nontrivial zero of the β function

$$\beta(g) = \left.\frac{\partial g}{\partial m}\right|_u. \tag{15}$$

The standard critical exponents are then obtained by evaluating the RG functions

$$\eta_\phi(g) = \left.\frac{\partial \ln Z_\phi}{\partial \ln m}\right|_u,$$

$$\eta_t(g) = \left.\frac{\partial \ln Z_t}{\partial \ln m}\right|_u, \tag{16}$$

at the fixed point g^*, i.e.,

$$\eta = \eta_\phi(g^*),$$

$$\frac{1}{\nu} = 2 + \eta_t(g^*) - \eta_\phi(g^*). \tag{17}$$

In three dimensions these RG functions are known to six loops for generic values of N [25,26]. For $N=0,1,2,3$, seven-loop series for η_ϕ and η_t were computed in Ref. [27].

In order to evaluate the crossover exponent ϕ_T associated with the operator $T_{ij}(x)$, we define the renormalization function $Z_T(g)$ from the one-particle irreducible two-point function $\Gamma_T^{(2)}(p)$ with an insertion of the operator T_{ij}, i.e., we set

$$\Gamma_T^{(2)}(0)_{ij;k,l} = Z_T^{-1}(g) A_{ijkl}, \tag{18}$$

where

$$A_{ijkl} = \delta_{ik}\delta_{jl} + \delta_{il}\delta_{jk} - \frac{2}{N}\delta_{ij}\delta_{kl}, \tag{19}$$

so that $Z_T(0)=1$. Then, we compute the RG function

$$\eta_T(g) = \left.\frac{\partial \ln Z_T}{\partial \ln m}\right|_u = \beta(g)\frac{d \ln Z_T}{dg} \tag{20}$$

and $\eta_T = \eta_T(g^*)$. Finally, the RG scaling relation

$$\phi_T = (2 + \eta_T - \eta)\nu \tag{21}$$

allows us to determine ϕ_T.

C. The fixed-dimension expansion: Six-loop results

We computed $\Gamma_T^{(2)}(0)$ to six loops. The calculation is rather cumbersome, since it requires the evaluation of 563 Feynman diagrams. We handled it with a symbolic manipulation program, which generates the diagrams and computes the symmetry and group factors of each of them. We used the numerical results compiled in Ref. [28] for the integrals associated with each diagram. We obtained

$$\begin{aligned}\eta_T(\bar{g}) = & -\bar{g}\frac{2}{8+N} + \bar{g}^2\frac{2(6+N)}{3(8+N)^2} - \bar{g}^3\frac{18.312\,844 + 3.433\,275N - 0.216\,745\,89N^2}{(8+N)^3} \\ & + \bar{g}^4\frac{140.799\,37 + 37.573\,408N + 1.036\,273\,6N^2 + 0.094\,342\,565N^3}{(8+N)^4} \\ & - \bar{g}^5\frac{1340.075 + 416.716\,57N + 17.622\,623N^2 - 0.911\,280\,56N^3 - 0.050\,833\,747N^4}{(8+N)^5} \\ & + \bar{g}^6\frac{15\,651.266 + 5665.6519N + 433.687\,12N^2 + 1.067\,550\,3N^3 + 0.679\,105\,59N^4 + 0.031\,393\,004N^5}{(8+N)^6} + O(\bar{g}^7),\end{aligned} \tag{22}$$

where, as usual, we have introduced the rescaled coupling $\bar{g}$ defined by

$$g = \frac{48\pi}{8+N}\bar{g}. \tag{23}$$

Field-theoretical perturbative expansions are divergent, and thus, in order to obtain accurate results, an appropriate resummation is required. We use the method of Ref. [29] that takes into account the large-order behavior of the perturbative expansion, see, e.g., Ref. [30]. Mean values and error bars are computed using the algorithm of Ref. [31].

Given the expansion of $\eta_T(\bar{g})$, we determine the perturbative expansion of $\phi_T(\bar{g})$, $\beta_T(\bar{g})$, and $\gamma_T(\bar{g})$, using the relations (10) and (21). For $N=2$, we obtain [32] $\phi_T = 1.176(4), 1.178(3)$, $\beta_T = 0.821(6), 0.825(5)$, and $\gamma_T = 0.355(2), 0.358(3)$, where, for each exponent, we report

TABLE I. Critical exponents associated with the tensor field $T_{ij}(x)$.

N	ϕ_T	β_T	γ_T
2	1.184(12)	0.830(12)	0.354(25)
3	1.271(21)	0.863(21)	0.41(4)
4	1.35(4)	0.90(4)	0.45(8)
5	1.40(4)	0.90(4)	0.50(8)
8	1.55(4)	0.94(4)	0.61(8)
16	1.75(6)	0.98(6)	0.77(12)

the estimate obtained from the direct analysis and from the analysis of the series of the inverse, i.e., from $1/\phi_T(g)$, etc. The two estimates obtained for each exponent agree within error bars, but, with the quoted errors, the scaling relations (10) are not well satisfied. For instance, using $\nu = 0.671\,55(27)$ (Ref. [33]) and $\beta_T = 0.823(6)$ we obtain $\phi_T = 1.192(6)$, while using the same value of ν and $\gamma_T = 0.3565(30)$ we have $\phi_T = 1.1855(15)$. These two estimates are slightly higher than those obtained from the analysis of $\phi_T(g)$ and $1/\phi_T(g)$. Clearly, the errors are somewhat underestimated, a phenomenon that is probably connected with the nonanalyticity [34–36] of the RG functions at the fixed point $\bar{g}^*$.

In order to obtain a conservative estimate, we have thus decided to take as estimate of ϕ_T the weighted average of the direct estimates and of the estimates obtained using β_T and γ_T together with the scaling relations [37]. The (very conservative) error is such to include all estimates. The other exponents are dealt with analogously. The final results for several values of N are reported in Table I.

D. Comparison with previous results

The exponent ϕ_T can also be computed in the ϵ expansion. Three-loop series were derived in Ref. [21],

$$\phi_T = 1 + \epsilon \frac{N}{2(N+8)} + \epsilon^2 \frac{N^3+24N^2+68N}{4(N+8)^3} + \epsilon^3 \frac{N^5+48N^4+788N^3+3472N^2+5024N-48N(5N+22)(N+8)\zeta(3)}{8(N+8)^5} + O(\epsilon^4). \tag{24}$$

The coefficients of this series decrease rapidly; for instance, we have

$$\phi_T(N=2) = 1 + 0.1\epsilon + 0.06\epsilon^2 - 0.007\,358\,99\epsilon^3 + O(\epsilon^4), \tag{25}$$

$$\phi_T(N=3) = 1 + 0.136\,364\epsilon + 0.083\,959\epsilon^2 + 0.000\,991\epsilon^3 + O(\epsilon^4), \tag{26}$$

for $N=2$ and 3, respectively. Thus, any resummation gives estimates that do not differ significantly from those obtained by simply setting $\epsilon=1$. For $N=2$ and 3 we obtain $\phi_T \approx 1.15$ and 1.22, in reasonable agreement—keeping into account that these are three-loop results—with the estimates of Table I. They are also in agreement with the estimate of Ref. [14] that reports $\phi_T = 1.16(7)$ for $N=2$, which has been obtained by analyzing the same $O(\epsilon^3)$ series and the two-loop series calculated in the framework of the fixed-dimension expansion.

The exponent ϕ_T has also been computed in the $1/N$ expansion [38] for $d=3$,

$$\phi_T = 2 - \frac{32}{\pi^2 N} + O\left(\frac{1}{N^2}\right). \tag{27}$$

For $N=16$ it gives $\phi_T = 1.80$, which agrees with the FT result of Table I.

The exponent ϕ_T has been estimated by high-temperature expansion techniques in Ref. [6], obtaining $\phi_T = 1.175(15)$ for $N=2$ and $\phi_T = 1.250(15)$ for $N=3$, in agreement with the FT estimates. For $N=5$, the exponent ϕ_T has also been determined by means of a Monte Carlo simulation [22], $\phi_T = 1.387(30)$.

Experimental estimates of ϕ_T are reported in Ref. [39]. We mention the experimental result $\phi_T = 1.17(2)$ for the $(2 \to 1+1)$ bicritical point in $GdAlO_3$ [40]. The $(3 \to 2+1)$ bicritical behavior has been studied in MnF_2 [41], obtaining $\phi_T = 1.279(31)$. The experimental results obtained for a nematic–smectic-A transition reported in Ref. [17] are $\beta_T = 0.76(4)$ and $\gamma_T = 0.41(9)$.

III. THE STRUCTURE FACTOR OF THE BILINEAR FIELDS IN THE HIGH-TEMPERATURE PHASE

A. Scaling behavior

The two-point correlation function of the fundamental field, i.e., $G(x) = \langle \vec{\phi}(0) \cdot \vec{\phi}(x) \rangle$, is of central importance because its Fourier transform $\widetilde{G}(q)$ is directly related to the scattering intensity in scattering experiments. For $t \to 0^+$, its asymptotic behavior is given by [42,43]

$$\widetilde{G}(q) = C^+ t^{-\gamma} f(q^2 \xi^2), \tag{28}$$

where C^+ is the amplitude of the magnetic susceptibility and the function $f(y)$ is universal. Taking the second-moment correlation length

$$\xi^2 \equiv \frac{1}{2d} \frac{\sum_x |x|^2 G(x)}{\sum_x G(x)} = -\widetilde{G}(0)^{-1} \left.\frac{\partial \widetilde{G}(q)}{\partial q^2}\right|_{q^2=0} \tag{29}$$

as length scale, the small-momentum behavior of $f(y)$ is $f(y) = 1/(1+y) + O(y^2)$, with very small $O(y^2)$ corrections. Theoretical results for the correlation function $\widetilde{G}(q)$ are reviewed, e.g., in Ref. [1].

In this section we study the scaling behavior of the two-point correlation functions of the bilinear fields $E(x)$ and $T_{ij}(x)$. Similar to the specific heat, which is given by the zero-momentum component of the two-point function $\widetilde{G}_E(q,t)$, the asymptotic behavior of $\widetilde{G}_{E,T}(q,t)$ for $t\to 0^+$ is not as simple as that of the fundamental two-point function. Indeed, in the scaling limit $t\to 0^+, q^2\to 0$ with $q^2\xi^2$ fixed, RG theory predicts

$$\widetilde{G}_{E,T}(q,t)=B_{E,T}[1+O(t)] +A^+_{E,T}t^{-\gamma_{E,T}}f_{E,T}(q^2\xi^2)[1+O(t^\Delta)], \quad (30)$$

where $B_{E,T}$ and $A^+_{E,T}$ are nonuniversal constants, $f_{E,T}(y)$ is a universal function satisfying $f_{E,T}(0)=1$, and Δ is the exponent related to the leading irrelevant operator. As amply discussed in textbooks—see, e.g., Ref. [30]—the presence of the background term B_E in the asymptotic behavior of $\widetilde{G}_E(q,t)$ is related to the need of an additive renormalization. One may easily see that the same argument applies to the two-point function $\widetilde{G}_T(q,t)$ of T_{ij}.

Since $\gamma_T>0$ for all $N\geqslant 2$, the leading behavior of the tensor two-point function is determined by the singular term depending on the scaling function $f_T(q^2\xi^2)$,

$$\widetilde{G}_T(q,t)=A^+_T t^{-\gamma_T}f_T(q^2\xi^2)[1+O(t^\Delta)+O(t^{\gamma_T})]. \quad (31)$$

The background term B_T gives subleading corrections of order t^{γ_T}, that turn out to be more relevant than the standard scaling corrections of order t^Δ. Indeed, for the physically relevant cases $N=2,3$, one finds that $\gamma_T<\Delta$ ($\Delta\approx 0.53$ for $N=2$ and $\Delta\approx 0.55$ for $N=3$, see, e.g., the results reviewed in Ref. [1]). The difference decreases as $N\to\infty$, since both γ_T and Δ converge to 1 with the same $1/N$ correction.

The same thing holds for the energy two-point function in the case of the Ising universality class for which α is positive, $\alpha=0.1199(7)$ (Ref. [44]), i.e.,

$$\widetilde{G}_E(q,t)=A^+_E t^{-\alpha}f_E(q^2\xi^2)[1+O(t^\Delta)+O(t^\alpha)], \quad (32)$$

where $\Delta\approx 0.53$, see, e.g., Ref. [45]. On the other hand, for the O(N) vector models with $N\geqslant 2$, since $\alpha<0$, the background term B_E gives the leading behavior of the energy two-point function $\widetilde{G}_E(q,t)$,

$$\widetilde{G}_E(q,t)=B_E+A^+_E t^{-\alpha}f_E(q^2\xi^2)[1+O(t^\Delta)]+O(t). \quad (33)$$

In these cases, the singular part vanishes for $t=0$ and is usually responsible for a cusplike finite maximum in the specific heat at the critical point, as it is observed in experiments and in lattice models. This requires the nonuniversal constant A^+_E to be negative (see the discussion in Sec. III C 1).

In order to single out the singular behavior, one may consider the derivative with respect to the reduced temperature t,

$$W_{E,T}(q,t)\equiv\frac{\partial \widetilde{G}_{E,T}}{\partial t}=-\gamma_{E,T}A^+_{E,T}t^{-1-\gamma_{E,T}}w_{E,T}(q^2\xi^2) \times[1+O(t^\Delta,t^{1+\gamma_{E,T}})], \quad (34)$$

where

$$w_{E,T}(y)=f_{E,T}(y)+\frac{2\nu}{\gamma_{E,T}}yf'_{E,T}(y)=1+O(y) \quad (35)$$

is another universal function.

1. Small-momentum behavior

At small momentum, i.e., for $y\equiv q^2\xi^2\ll 1$, the scaling functions $f_{E,T}(y)$ behave as

$$f_E(y)=1+\sum_{n=1} e_n y^n, \quad (36)$$

$$f_T(y)=1+\sum_{n=1} a_n y^n. \quad (37)$$

Using Eq. (35), these expansions can be related to those of the scaling functions $w_{E,T}(y)$,

$$w_E(y)=1+\sum_{n=1} \overline{e}_n y^n, \quad (38)$$

$$w_T(y)=1+\sum_{n=1} \overline{a}_n y^n. \quad (39)$$

Indeed, it is immediate to obtain

$$\overline{e}_n=e_n\left(1+\frac{2n\nu}{\alpha}\right), \quad (40)$$

$$\overline{a}_n=a_n\left(1+\frac{2n\nu}{\gamma_T}\right). \quad (41)$$

Simple arguments based on perturbation theory suggest that the convergence radius R_c of the small-momentum expansions is determined by the two-particle cut. The singularity in the complex plane closest to the origin is expected to be $y_s=-4S^+_M$, where $S^+_M=\xi^2/\xi^2_{\rm gap}$ and $\xi_{\rm gap}$ is the exponential correlation length that determines the large-distance exponential behavior of the fundamental two-point function. Therefore, $R_c=4S^+_M$. For the O(N) vector models, S^+_M is very close to 1, so that $R_c\approx 4$. For example, $S^+_M=0.999\,601(6)$ for the Ising universality class [44], $S^+_M=0.999\,592(6)$ for the XY universality class [33], $S^+_M=0.999\,59(4)$ for the Heisenberg universality class [46], and $S^+_M=1-0.004\,590/N+O(1/N^2)$ in the large-N limit [46]. As a consequence, for $n\to\infty$,

$$\frac{e_{n+1}}{e_n}\approx\frac{a_{n+1}}{a_n}\approx\frac{\overline{e}_{n+1}}{\overline{e}_n}\approx\frac{\overline{a}_{n+1}}{\overline{a}_n}\approx-\frac{1}{4}. \quad (42)$$

The constants e_1 and a_1 are related to the universal ratios $X_{E,T} \equiv \xi^2_{E,T}/\xi^2$ introduced in Refs. [11,18], where $\xi_{E,T}$ are the second-moment correlation lengths associated with the singular part of the energy and of the tensor two-point functions, respectively. More precisely, if $\gamma_{T,E}>0$, the correlation length is defined by Eq. (29), replacing $\widetilde{G}(q)$ with $\widetilde{G}_{E,T}(q)$. If the exponent is negative, then

$$\xi_E^2 = -(\widetilde{G}_E(0) - B_E)^{-1} \frac{\partial \widetilde{G}_E(q)}{\partial q^2}\bigg|_{q^2=0}. \tag{43}$$

The universal ratios X_E and X_T are given by $X_E = -e_1$ and $X_T = -a_1$.

2. Large-momentum behavior

The large-momentum behavior of the fundamental correlation function is given by the Fisher-Langer formula [47],

$$f(y) \approx \frac{A_1}{y^{1-\eta/2}}\left(1 + \frac{A_2}{y^{(1-\alpha)/(2\nu)}} + \frac{A_3}{y^{1/(2\nu)}}\right). \tag{44}$$

One may derive a similar expression for the correlation functions of the bilinear fields. The large-momentum behavior of the structure factors can be studied by performing a short-distance expansion of the two-point functions $G_E(x)$ and $G_T(x)$. Following the method outlined in Ref. [48], we obtain the corresponding asymptotic expansions for $y \to \infty$,

$$f_E(y) \approx E_1 y^{-\alpha/(2\nu)}\left(1 + \frac{E_2}{y^{(1-\alpha)/(2\nu)}} + \frac{E_3}{y^{1/(2\nu)}}\right), \tag{45}$$

$$f_T(y) \approx T_1 y^{-\gamma_T/(2\nu)}\left(1 + \frac{T_2}{y^{(1-\alpha)/(2\nu)}} + \frac{T_3}{y^{1/(2\nu)}}\right). \tag{46}$$

The derivation of these formulas is reported in Appendix A. Notice that for the O(N) vector models with $N \geqslant 2$, since $\alpha < 0$, $f_E(y)$ increases as $y \to \infty$.

B. Field-theory calculations: Generalities

Because of the presence of the background term, the FT calculation of the scaling functions $f_E(y)$ and $f_T(y)$ requires some care. First, we define the dimensionless functions

$$\mathcal{G}_{E,T}(g,y) \equiv u \widetilde{G}_{E,T}(q,t,u), \tag{47}$$

where g is the four-point renormalized coupling. Then, in order to eliminate the constant additive renormalization term, we consider the derivative with respect to m of $\mathcal{G}_{E,T}(g,y)$,

$$\mathcal{W}_{E,T}(g,y) = m\frac{\partial}{\partial m}\mathcal{G}_{E,T}(g,y)\bigg|_u = \beta(g)\frac{\partial \mathcal{G}_{E,T}(g,y)}{\partial g} - 2y\frac{\partial \mathcal{G}_{E,T}(g,y)}{\partial y}. \tag{48}$$

TABLE II. Estimates of the coefficients $\overline{e_i}$ for several values of N.

N	$\overline{e_1}$	$\overline{e_2}/\overline{e_1}$	$\overline{e_3}/\overline{e_2}$	$\overline{e_4}/\overline{e_3}$	$\overline{e_5}/\overline{e_4}$
1	−0.170(5)	−0.206(1)	−0.221(1)	−0.229(1)	−0.234(1)
2	−0.155(5)	−0.199(1)	−0.216(2)	−0.226(2)	−0.232(2)
3	−0.142(5)	−0.193(2)	−0.213(2)	−0.222(2)	−0.230(3)
4	−0.133(6)	−0.189(3)	−0.211(2)	−0.222(3)	−0.228(3)
5	−0.126(6)	−0.186(3)	−0.209(3)	−0.221(3)	−0.228(4)
8	−0.111(5)	−0.180(3)	−0.206(3)	−0.219(4)	−0.227(4)

At the fixed point g^*, the functions $\mathcal{W}_{E,T}(g,y)$ differ from $W_{E,T}(q,t)$, defined in Eq. (34), by a multiplicative factor independent of q. Therefore, the scaling functions $w_{E,T}(g,y)$, defined in Eq. (35), are given by

$$w_{E,T}(g,y) = \frac{\mathcal{W}_{E,T}(g,y)}{\mathcal{W}_{E,T}(g,0)}. \tag{49}$$

Note that the zero-momentum functions $\mathcal{W}_{E,T}(g,0)$ are related to the exponents $\gamma_{E,T}$ by the relation

$$-\frac{\gamma_{E,T}}{\nu} = \lim_{g\to g^*} \beta(g)\frac{d \ln \mathcal{W}_{E,T}(g,0)}{dg}. \tag{50}$$

C. Field-theoretical results

1. Small-momentum expansion

We compute the small-momentum expansion of the structure factors to four loops in the fixed-dimension approach and to three loops in the ϵ expansion.

In the fixed-dimension approach, we first determine the expansion in powers of g of the coefficients $\overline{e_i}$ and $\overline{a_i}$ defined in Eqs. (38) and (39). The explicit expressions are reported in Appendix B. In order to obtain numerical estimates we use the same resummation procedure outlined in the preceding section. Our numerical results are presented in Tables II and III. Note that, as expected, the ratios $\overline{e_{i+1}}/\overline{e_i}$ and $\overline{a_{i+1}}/\overline{a_i}$ quickly approach $-1/4$. The corresponding coefficients e_i and a_i are obtained by using the relations (40) and (41). For the exponent ν we use the same values reported before [37], while for γ_T we use the results of Table I. In the case of a_i a large part of the uncertainty is due to the error in the exponent γ_T that enters the relation between $\overline{a_i}$ and a_i. The re-

TABLE III. Estimates of the coefficients $\overline{a_i}$ for several values of N.

N	$\overline{a_1}$	$\overline{a_2}/\overline{a_1}$	$\overline{a_3}/\overline{a_2}$	$\overline{a_4}/\overline{a_3}$	$\overline{a_5}/\overline{a_4}$
2	−0.203(2)	−0.224(2)	−0.232(1)	−0.236(1)	−0.239(1)
3	−0.208(2)	−0.226(1)	−0.234(1)	−0.238(1)	−0.240(1)
4	−0.213(2)	−0.228(1)	−0.235(1)	−0.239(1)	−0.241(1)
5	−0.216(1)	−0.230(1)	−0.236(1)	−0.240(1)	−0.242(1)
8	−0.224(1)	−0.235(1)	−0.239(1)	−0.242(1)	−0.244(1)

TABLE IV. Results of the coefficients e_i and a_i for several values of N and from various analyses: (a) ($d=3$) by using the fixed-dimension results for $\overline{e_i}$ and $\overline{a_i}$, and by directly analyzing the series for a_i; (b) (ϵ expan) by resummation of the three-loop ϵ expansion.

N	i	e_i $(d=3)_{\text{from } \overline{e_i}}$	a_i $(d=3)_{\text{from } \overline{a_i}}$	a_i $(d=3)_{\text{direct}}$	e_i (ϵ expan)	a_i (ϵ expan)
1	1	$-0.0137(2)$			$-0.0145(11)$	
	2	$0.147(3)\times10^{-2}$			$0.17(2)\times10^{-2}$	
	3	$-0.219(4)\times10^{-3}$			$-0.26(3)\times10^{-3}$	
	4	$0.38(1)\times10^{-4}$			$0.47(6)\times10^{-4}$	
	5	$-0.71(1)\times10^{-5}$			$-0.9(1)\times10^{-5}$	
2	1	$0.0017(1)$	$-0.042(2)$	$-0.042(1)$	$0.000(2)$	$-0.041(2)$
	2	$-0.017(1)\times10^{-2}$	$0.530(3)\times10^{-2}$	$0.52(1)\times10^{-2}$	$0.00(3)\times10^{-2}$	$0.48(3)\times10^{-2}$
	3	$0.024(2)\times10^{-3}$	$-0.85(1)\times10^{-3}$	$-0.84(3)\times10^{-3}$	$0.00(5)\times10^{-3}$	$-0.75(6)\times10^{-3}$
	4	$-0.041(2)\times10^{-4}$	$1.5(2)\times10^{-4}$	$1.5(1)\times10^{-4}$	$0.0(1)\times10^{-4}$	$1.3(1)\times10^{-4}$
	5	$0.076(4)\times10^{-5}$	$-3.0(2)\times10^{-5}$	$-3.0(2)\times10^{-5}$	$0.0(2)\times10^{-5}$	$-2.6(2)\times10^{-5}$
3	1	$0.015(2)$	$-0.047(4)$	$-0.0465(8)$	$0.012(2)$	$-0.045(1)$
	2	$-0.14(2)\times10^{-2}$	$0.59(5)\times10^{-2}$	$0.59(1)\times10^{-2}$	$-0.13(3)\times10^{-2}$	$0.54(3)\times10^{-2}$
	3	$0.19(2)\times10^{-3}$	$-0.96(9)\times10^{-3}$	$-0.96(2)\times10^{-3}$	$0.19(5)\times10^{-3}$	$-0.85(5)\times10^{-3}$
	4	$-0.32(4)\times10^{-4}$	$1.8(2)\times10^{-4}$	$1.75(7)\times10^{-4}$	$-0.3(1)\times10^{-4}$	$1.5(1)\times10^{-4}$
	5	$0.6(1)\times10^{-5}$	$-3.4(3)\times10^{-5}$	$-3.4(2)\times10^{-5}$	$0.6(2)\times10^{-5}$	$-2.9(2)\times10^{-5}$
4	1	$0.026(1)$	$-0.05(1)$	$-0.0500(6)$	$0.022(2)$	$-0.049(1)$
	2	$-0.23(1)\times10^{-2}$	$0.63(9)\times10^{-2}$	$0.645(5)\times10^{-2}$	$-0.22(3)\times10^{-2}$	$0.60(2)\times10^{-2}$
	3	$0.31(1)\times10^{-3}$	$-1.0(2)\times10^{-3}$	$-1.06(2)\times10^{-3}$	$0.33(4)\times10^{-3}$	$-0.94(4)\times10^{-3}$
	4	$-0.50(2)\times10^{-4}$	$1.9(3)\times10^{-4}$	$1.96(6)\times10^{-4}$	$-0.6(1)\times10^{-4}$	$1.7(1)\times10^{-4}$
	5	$0.91(3)\times10^{-5}$	$-3.7(6)\times10^{-5}$	$-3.9(2)\times10^{-5}$	$1.1(2)\times10^{-5}$	$-3.3(1)\times10^{-5}$
5	1	$0.030(1)$	$-0.053(6)$	$-0.0533(4)$	$0.029(2)$	$-0.0528(3)$
	2	$-0.25(1)\times10^{-2}$	$0.7(1)\times10^{-2}$	$0.699(5)\times10^{-2}$	$-0.30(2)\times10^{-2}$	$0.65(2)\times10^{-2}$
	3	$0.34(1)\times10^{-3}$	$-1.2(2)\times10^{-3}$	$-1.16(2)\times10^{-3}$	$0.44(4)\times10^{-3}$	$-1.03(3)\times10^{-3}$
	4	$-0.55(2)\times10^{-4}$	$2.1(3)\times10^{-4}$	$2.15(5)\times10^{-4}$	$-0.8(1)\times10^{-4}$	$1.85(5)\times10^{-4}$
	5	$1.00(3)\times10^{-5}$	$-4.2(6)\times10^{-5}$	$-4.3(2)\times10^{-5}$	$1.4(2)\times10^{-5}$	$-3.6(1)\times10^{-5}$
8	1	$0.047(1)$	$-0.060(6)$	$-0.0602(1)$	$0.046(2)$	$-0.061(1)$
	2	$-0.35(1)\times10^{-2}$	$0.8(1)\times10^{-2}$	$0.817(5)\times10^{-2}$	$-0.43(1)\times10^{-2}$	$0.77(1)\times10^{-2}$
	3	$0.45(1)\times10^{-3}$	$-1.4(2)\times10^{-3}$	$-1.40(2)\times10^{-3}$	$0.62(2)\times10^{-3}$	$-1.24(2)\times10^{-3}$
	4	$-0.72(2)\times10^{-4}$	$2.6(3)\times10^{-4}$	$2.58(4)\times10^{-4}$	$-1.05(3)\times10^{-4}$	$2.24(4)\times10^{-4}$
	5	$1.28(4)\times10^{-5}$	$-5.1(6)\times10^{-5}$	$-5.1(2)\times10^{-5}$	$1.95(5)\times10^{-5}$	$-4.4(1)\times10^{-5}$

sults are reported in Table IV. We also performed direct analyses of the coefficients e_i, a_i, considering the g series that can be obtained from Eqs. (40) and (41). The results are substantially consistent with those obtained by first estimating $\overline{e_i}$ and $\overline{a_i}$. In the case of a_i they turn out to be more precise; we also show them in Table IV (third column of results).

In ϵ expansion we directly resum the expansions of e_i and a_i reported in Appendix B. The results are also reported in Table IV and are in substantial agreement with the fixed-dimension results. For a_1, we also perform a constrained analysis that makes use of the available results for a_1 in two and one dimensions. Such a method was introduced in Ref. [49] and generalized in Refs. [34,50]. In many instances it has provided quite accurate results for critical quantities. We use the estimates of a_1 in two dimensions reported in Refs. [51,52], $a_1=-0.0812(5)$, $-0.1014(6)$, and $-0.1313(9)$ for $N=3,4,8$, respectively. We also make use of the one-dimensional result [53], $a_1=-(N-1)^2/(4N^2)$. From the analysis constrained in one dimension, in three dimensions we obtain $a_1=-0.0397(2)$ for $N=2$ and $a_1=-0.0533(3)$ for $N=5$, while from the analysis constrained in two dimensions we obtain $a_1=-0.0460(3)$ for $N=3$, $a_1=-0.0507(5)$ for $N=4$, $a_1=-0.0621(2)$ for $N=8$. Constraining the analysis both in two and one dimension, we obtain $a_1=-0.0458(1)$ for $N=3$, $a_1=-0.0514(6)$ for $N=4$, $a_1=-0.0625(2)$ for $N=8$. These results are compatible with those of Table IV.

TABLE V. Final estimates of the coefficients e_1 and a_1.

N	e_1	a_1
1	$-0.0140(5)$	
2	$0.0017(1)$	$-0.041(2)$
3	$0.014(3)$	$-0.046(1)$
4	$0.024(3)$	$-0.051(2)$
5	$0.030(1)$	$-0.0533(5)$
8	$0.047(1)$	$-0.062(2)$

Taking into account the above-reported results for e_1 and a_1, we consider as final estimates the numbers reported in Table V. The errors are rather conservative and are such to include all the results we have obtained.

As already noted in Ref. [11], $e_1 = -\alpha/(6\gamma) + O(\epsilon^3)$ and $a_1 = -\gamma_T/(6\gamma) + O(\epsilon^3)$. These relations are not satisfied to order ϵ^3, see Appendix B. Nonetheless, they still provide very good approximations to e_1 and a_1. For instance (see Ref. [1] for the estimates of the critical exponents), $-\alpha/(6\gamma) = -0.01377(8), 0.00185(10), 0.0159(8)$, respectively, for $N=1,2,3$, where the error is related to the uncertainty on the estimates of α and γ.

The coefficient e_1 has also been computed for $N=1$ by Monte Carlo simulations [54]. The numerical data are well described by $-\alpha_{\rm eff}(t)/[6\gamma_{\rm eff}(t)]$, where $\alpha_{\rm eff}(t)$ and $\gamma_{\rm eff}(t)$ are effective exponents determined from the specific heat and the susceptibility.

It is interesting to note that the signs of a_i and e_i are strictly related to the signs of the amplitudes $A^+_{E,T}$ and of the exponents α and γ_T. First, we observe that in the critical limit the correlation functions are non-negative, i.e., $G_{E,T}(x) \geqslant 0$. Indeed, the lattice ϕ^4 model with nearest-neighbor couplings is exactly reflection positive and, therefore, the above-reported inequalities are rigorously true for any value of the couplings. At criticality, they should hold for any model in the same universality class. Therefore, all moments are positive, i.e., $\Sigma_x |x|^{2n} G_{E,T}(x) \geqslant 0$. If the correlation functions have the scaling forms (31) and (32), this implies

$$A^+_{E,T} \geqslant 0, \quad (-1)^n a_n \geqslant 0. \tag{51}$$

For $N \geqslant 2$, using Eq. (33), we obtain

$$B_E \geqslant 0, \quad (-1)^n A^+_E e_n \geqslant 0. \tag{52}$$

Relations (51) are satisfied by our results, while Eq. (52) and our result $e_1 > 0$ imply $A^+_E < 0$. Thus, although $A^+_{E,T}$ is nonuniversal, the positivity (unitarity in FT language) of the theory fixes its sign.

As a final remark, note that a_1 and e_1 are very small. The values of a_1 are quite smaller than what would be naively expected. The nearest singularity in the complex y plane corresponds to the two-particle cut, thus at large distance $G_T(x) \sim |x|^q \exp(-|x|/\xi'_T)$ with $\xi'_T = \xi_{\rm gap}/2$, where $\xi_{\rm gap}$ is the exponential correlation length that determines the large-distance exponential behavior of the fundamental two-point function. Then, positivity of $G_T(x)$ requires the second-moment correlation length ξ_T to be smaller than ξ'_T. As a consequence, since $\xi_{\rm gap} \approx \xi$ (see Sec. III A 1), $|a_1| \lesssim 1/4$. But this bound turns out to be much larger than the actual value of a_1.

2. Large-momentum expansion

We also compute the constants E_i and T_i of the large-momentum behavior of $f_{E,T}(y)$. Matching the large-momentum expansion of the two-loop expression of $\widetilde{G}_{E,T}(q,t)$ with Eqs. (45) and (46), we obtain

$$E_1 = 1 + \frac{4-N}{8+N}\epsilon + O(\epsilon^2), \tag{53}$$

$$E_2 = -2 + \frac{2(5+N)}{8+N}\epsilon + E_{22}\epsilon^2 + O(\epsilon^3),$$

$$E_3 = 2 - \frac{14+N}{8+N}\epsilon + E_{32}\epsilon^2 + O(\epsilon^3),$$

and

$$T_1 = 1 + \frac{4+N}{8+N}\epsilon + O(\epsilon^2), \tag{54}$$

$$T_2 = -\frac{2(4+N)}{4-N} + \frac{2(4+N)(20-13N-N^2)}{(4-N)^2(8+N)}\epsilon + T_{23}\epsilon^2 + O(\epsilon^3),$$

$$T_3 = \frac{2(4+N)}{4-N} - \frac{(4+N)(56-34N-N^2)}{(4-N)^2(8+N)}\epsilon + T_{33}\epsilon^2 + O(\epsilon^3).$$

Moreover,

$$E_{22} + E_{32} = -\frac{(N^3 - 14N^2 - 140N - 432)}{2(N+8)^3} + \frac{N-4}{12(N+8)}\pi^2,$$

$$T_{22} + T_{32} = -\frac{(N+4)(N^2+14N+108)}{2(N+8)^3} - \frac{N+4}{12(N+8)}\pi^2. \tag{55}$$

The constants E_1 and T_1 are in agreement with the results of Ref. [11]. The divergence of the coefficients T_2 and T_3 for $N \to 4$ is related to the vanishing of the $O(\epsilon)$ term in the expansion of α [55].

The large size of the coefficients makes it difficult to resum the perturbative series. For the physically interesting case of $N=2$ we report the result obtained by setting $\epsilon=1$ and give as error the size of the last coefficient. In this way we obtain, $E_1 = 1.3(3)$, $E_2 = -0.7(1.3)$, and $E_3 = 0.3(1.7)$ for $N=1$, and $E_1 = 1.2(2)$, $E_2 = -0.6(1.4)$, $E_3 = 0.4(1.6)$, $T_1 = 1.6(6)$, $T_2 = -9(3)$, $T_3 = 8.4(2.4)$ for $N=2$. Moreover, $E_2 + E_3 = 0.0(2)$ and $T_2 + T_3 = -0.7(1)$ for $N=2$.

D. Interpolations of the structure factors

In Ref. [11] the authors discuss several approximate forms for $f_{E,T}(y)$. They present generalizations of the Fisher-Burford [42] approximant for $\langle \phi\phi \rangle$. These approximations are quite crude and do not reproduce the full Fisher-Langer behavior for large y. A better approach based on dispersion theory was put forward by Bray [24]. Here, we will apply the same method to the universal functions $f_E(y)$ and $f_T(y)$.

A generalization of the arguments presented in Ref. [24] gives the following representation for $f_T(y)$:

$$f_T(y)=1-\frac{yT_1}{\pi}\sin\left(\frac{\pi\gamma_T}{2\nu}\right)\int_{4S_M^+}^{\infty}dx\,\frac{x^{-1-\gamma_T/(2\nu)}}{x+y}F_T(x), \tag{56}$$

where $F_T(x)$ is the spectral function satisfying $F_T(\infty)=1$. We assume here that the only singularities of $f_T(y)$ in the complex plane are branch cuts on the negative real axis and that the leading one corresponds to the two-particle state, so that the disk $|y|<4S_M^+$ is free of singularities. Under this assumption, the representation (56) is exact.

For generic $F_T(x)$, Eq. (56) does not give the correct Fisher-Langer behavior (46). Indeed, for $y\to\infty$ we obtain $f_T(y)\approx\text{const}+T_1y^{-\gamma_T/(2\nu)}$. We must thus require the constant to be zero. This gives the sum rule

$$\frac{T_1}{\pi}\sin\left(\frac{\pi\gamma_T}{2\nu}\right)\int_{4S_M^+}^{\infty}dx\,x^{-1-\gamma_T/(2\nu)}F_T(x)=1, \tag{57}$$

which allows the determination of T_1 once $F_T(x)$ is given.

Equation (56) applies also to $f_E(y)$ with the obvious replacements. However, the sum rule (57) requires $\alpha>0$ and can thus be used only in the Ising case. For $\alpha<0$, Eq. (57) is replaced by

$$\frac{E_1}{\pi}\sin\left(\frac{\pi\alpha}{2\nu}\right)\left[\frac{2\nu}{\alpha}(4S_M^+)^{-\alpha/(2\nu)}+\int_{4S_M^+}^{\infty}dx\,x^{-1-\alpha/(2\nu)}(F_E(x)-1)\right]=1. \tag{58}$$

In order to obtain approximate expressions for the structure factors, we must assume a specific form for the spectral function. For this purpose, we assume, as in Ref. [24], that $F_T(x)$ gives the exact Fisher-Langer behavior on the cut. Explicitly, we consider

$$F_T(x)=1+T_2x^{-(1-\alpha)/(2\nu)}\left[\cos\frac{\pi(1-\alpha)}{2\nu}+\sin\frac{\pi(1-\alpha)}{2\nu}\cot\frac{\pi\gamma_T}{2\nu}\right]+T_3x^{-1/(2\nu)}\left[\cos\frac{\pi}{2\nu}+\sin\frac{\pi}{2\nu}\cot\frac{\pi\gamma_T}{2\nu}\right]. \tag{59}$$

To completely determine the spectral function, we must specify the constants T_2 and T_3. We use here the ϵ-expansion results of Sec. III C. These estimates are not very precise, but the interpolation is quite insensitive on T_2 and T_3 separately. Indeed, what really matters is their sum T_2+T_3 that is more accurately determined. In order to test these interpolations, we can compare the estimates of T_1 and a_i—and, analogously, of E_1 and e_i—with those of the preceding sections. For $N=2$, using $T_2=-9$ and $T_3=8.4$, we obtain $T_1\approx1.56$, $a_1\approx-0.055$, $a_2\approx0.008$, which are reasonably close to the estimates reported before. Analogously, using $E_2=-0.6$ and $E_3=0.4$, we obtain $E_1\approx1.00$, $e_1\approx0.005$, and $e_2\approx-0.0007$, again in reasonable agreement with previous results. In particular, the fact that $|e_1|\ll|a_1|$ is correctly predicted by the approximation. For $N=1$, using $E_2=-2/3$, $E_3=1/3$, we obtain $E_1\approx1.20$, $e_1\approx-0.016$, $e_2\approx0.0019$, in reasonable agreement with what is reported above.

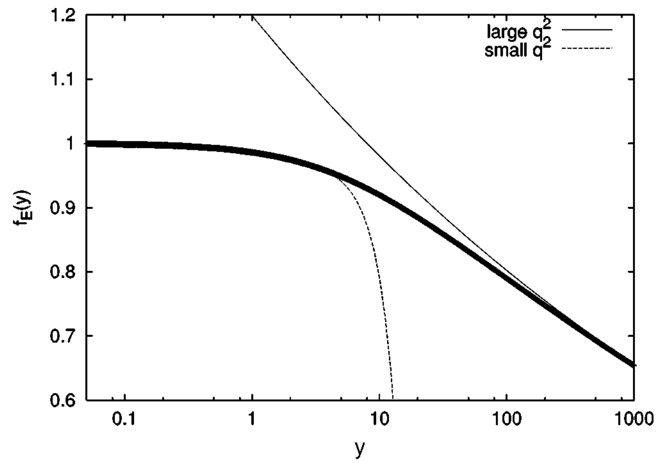

FIG. 1. Universal function $f_E(y)$ obtained using Eqs. (56) and (59) for $N=1$. We also report the large-y behavior, $f_E(y)\approx1.199y^{-0.087\,25}$ and the small-y behavior, $f_E(y)\approx1-0.013\,66y+0.001\,467y^2-0.000\,219y^3$.

In Fig. 1 we report $f_E(y)$ for $N=1$ and in Figs. 2 and 3 a graph of $f_E(y)$ and of $f_T(y)$ for $N=2$. It is interesting to note that for $N=2$ the function $f_E(y)$ varies slowly and differs from one only for quite large values of y. Taking also into account that the prefactor vanishes as $t\to0$, the q^2 dependence of $\tilde{G}_E(q,t)$ should be hardly visible in experiments and in numerical Monte Carlo simulations. Moreover, in this case $f_E(y)\geqslant1$ for all y, so that, because of the inequalitites (52), there is an attenuation of the singular behavior for increasing q, as generally expected.

IV. EXPERIMENTAL APPLICATIONS

In this section we briefly discuss the applications to some physical systems.

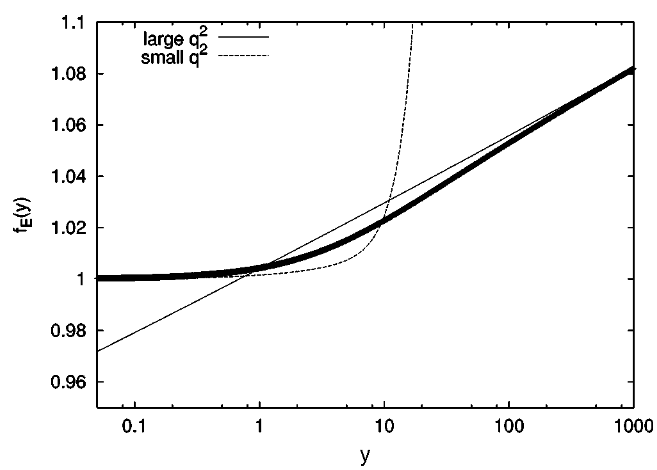

FIG. 2. Universal function $f_E(y)$ obtained using Eqs. (56) and (59) for $N=2$. We also report the large-y behavior, $f_E(y)\approx1.00y^{0.010\,908}$ and the small-y behavior, $f_E(y)\approx1+0.001\,71y-0.000\,169y^2+0.000\,0243y^3$.

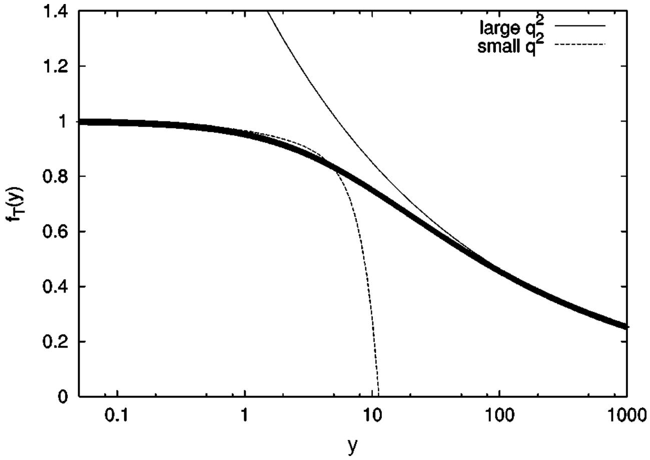

FIG. 3. Universal function $f_T(y)$ obtained using Eqs. (56) and (59) for $N=2$. We also report the large-y behavior, $f_T(y) \approx 1.559 y^{-0.263\,569}$ and the small-y behavior, $f_T(y) \approx 1 - 0.0397y + 0.0053y^2 - 0.000\,852 y^3$.

As already mentioned in the Introduction, the crossover exponent ϕ_T associated with the traceless tensor field $T_{ij}(x)$ describes the instability of the O(N)-symmetric theory against anisotropy [2–5]. It is thus relevant for the description of multicritical phenomena, for instance, the critical behavior near a bicritical point where two critical lines with O(N) and O(M) symmetry meet, showing a critical behavior with enlarged O($N+M$) symmetry, see, e.g., Refs. [6–8]. Physical realizations of bicritical points are provided by antiferromagnets in a magnetic field H. For instance, in the T-H plane uniaxial antiferromagnetic spin systems may present two lines of continuous transitions, characterized by an Ising and XY critical behavior, respectively, that meet at a point, where the symmetry is enlarged to O(3). The crossover exponent ϕ_T is relevant to describe the behavior of the system in the neighborhood of the O(3) symmetric point, see, e.g., Ref. [8].

Another interesting example of bicritical point appears in the recent SO(5) theory of high-T_c superconductivity [9]. According to this theory, the SO(5) symmetry should be realized at a bicritical point, where two critical lines merge: one is related to the antiferromagnetic properties and is characterized by an SO(3) symmetry and the other is associated with superconductivity and has U(1) symmetry. Actually, this issue is still debated, since it is not clear whether the SO(5) symmetric fixed point is really stable. On the one hand, Monte Carlo simulations reported in Ref. [22] support its stability. On the other hand, Ref. [56] presents solid arguments showing that another fixed point, i.e., the tetracritical decoupled fixed point, is stable. These two facts are not necessarily in contradiction, since one cannot exclude the presence of two stable fixed points, although experience suggests that this possibility is rather unlikely.

Many physical systems exhibit phase transitions characterized by the establishment of a density wave. The order parameter of density waves in a uniaxial system is the complex amplitude ϕ_1, associated with the contribution $\mathrm{Re}\,\phi_1 e^{iq_0 z}$ to the density modulation, where q_0 is the wavelength of the modulation. The critical behavior is then expected to be described by the XY universality class. Interesting examples in solids are charge-density wave systems, see, e.g., Refs. [57,58]. In three-dimensional complex fluids the density-wave phenomenon occurs at the nematic–smectic-A phase transition, which corresponds to the establishment of a one-dimensional mass-density wave along the direction of the orientational order. Beside the order parameter ϕ_1, also higher harmonics, associated with the contribution $\mathrm{Re}\,\phi_n e^{inq_0 z}$ to the density, are expected to show a critical behavior, which is essentially induced by the critical behavior of the fundamental field ϕ_1. Indeed, according to the theory reported in Refs. [11,18], the average density modulation $\langle \phi_n \rangle$ associated with the wave vector $nq_0\hat{z}$ should be proportional to $\langle \phi_1^n \rangle$, thus showing a singular behavior $\langle \phi_1^n \rangle \sim t^{\beta_n}$, where $\beta_n = 2 - \alpha - \phi_n$ and ϕ_n is the crossover exponent associated with the nth-order anisotropy at the XY fixed point. In the case $n=2$, i.e., the second harmonic, the relevant operator is the traceless tensor operator T_{ij}, cf. Eq. (3), thus $\beta_2 = \beta_T$. The same theory predicts that the leading critical contribution to the structure factor

$$S_n(q) = \int d^3x\, e^{iqx} \langle \phi_n(0)^* \phi_n(x) \rangle \tag{60}$$

is proportional to

$$G_n(q) = \int d^3x\, e^{iqx} \langle \phi_1^n(0)^* \phi_1^n(x) \rangle. \tag{61}$$

In the case of the second harmonic, $G_2(q) = G_T(q)$, whose scaling behavior has been determined in Sec. III. Some experimental results have been reported in Ref. [17], and reanalyzed in Ref. [14]. The small value of $X_T = -a_1$ is crucial to provide an explanation [11,18], consistently with RG theory, of the experimental results of Ref. [17].

As discussed in Ref. [11], the correlations $G_{E,T}$ of quadratic operators are also relevant in the description of certain liquid and solids, where an effective coupling between the order parameter and elastic deformations occurs, and may be measured by sound-attenuation experiments. In these systems, for symmetry reasons, the lowest-order coupling is expected to be linear in the strain and quadratic in the order parameter. A more thorough discussion can be found in Ref. [11].

Applications to polymers have been recently discussed in Ref. [59].

APPENDIX A: LARGE-MOMENTUM BEHAVIOR FOR THE BILINEAR CORRELATION FUNCTIONS

In this appendix, we compute the large-momentum behavior of the correlation function. We follow closely the discussion of Refs. [48,60] for the correlation function of the field ϕ.

1. The energy correlation function

The basic ingredient of the calculation is the short-distance expansion of the product of operators $E(x+y/2)E(x-y/2)$. For $y\to 0$, see, e.g., Ref. [30], this product is equal to the sum of all the operators that are allowed by symmetries, multiplied by C-number coefficients, that take into account the short-distance behavior. The most singular contribution comes from the operators of smallest dimension. In this case, neglecting the contribution related to the identity operator, it implies

$$E(x+y/2)E(x-y/2) = C(y)E(x) + (\text{less singular contributions}). \tag{A1}$$

Now, let us consider the connected correlation function of l composite operators $E(x)$, $G^{(l)}(p_1,\ldots,p_l)$, and its renormalized counterpart $G_R^{(l)}(p_1,\ldots,p_l) = Z_t^l Z_\phi^{-l} G^{(l)}(p_1,\ldots,p_l)$. Then, Eq. (A1) implies for $p \gg m$

$$G_R^{(l)}(p,-p,0,\ldots,0) \approx \tilde{C}(p;m) G_R^{(l-1)}(0,\ldots,0), \tag{A2}$$

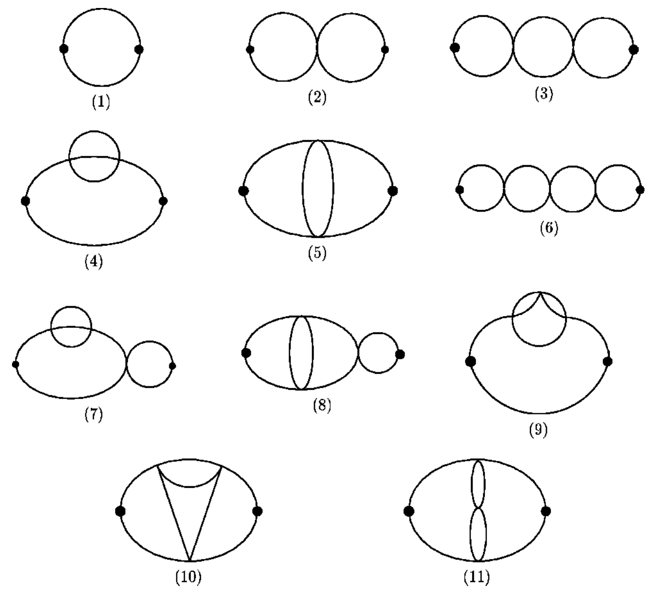

FIG. 4. Feynman diagrams contributing in the four-loop computation of the two-point functions $G_{E,T}$. The black blobs indicate the insertion of the bilinear operators.

TABLE VI. For each diagram j contributing to the energy and tensor two-point function we report: the number of loops l, the symmetry factor S_j, the group factors $C_j^{E,T}$, and the expansion of the integral $I_j(y)$ in fixed dimension $d=3$.

j	l	S_j	$\frac{C_j^E}{N}$	$\frac{4C_j^T}{N(N-1)}$	$(8\pi)^l I_j(y)$
1	1	2	1	2	$\frac{2}{\sqrt{y}}\arctan\frac{\sqrt{y}}{2}$
2	2	1	$\frac{2+N}{3}$	$\frac{4}{3}$	I_1^2
3	3	$\frac{1}{2}$	$\frac{(2+N)^2}{9}$	$\frac{8}{9}$	I_1^3
4	3	$\frac{2}{3}$	$\frac{2+N}{3}$	$\frac{2(2+N)}{3}$	$-0.0376821+0.00160802y+0.000209975y^2 -0.00012236y^3+0.0000404108y^4 -0.0000116689y^5+O(y^6)$
5	3	1	$\frac{2+N}{3}$	$\frac{2(6+N)}{9}$	$0.5-0.105903y+0.0222193y^2-0.00477681y^3 +0.00104957y^4-0.000234591y^5+O(y^6)$
6	4	$\frac{1}{4}$	$\frac{(2+N)^3}{27}$	$\frac{16}{27}$	I_1^4
7	4	$\frac{2}{3}$	$\frac{(2+N)^2}{9}$	$\frac{4(2+N)}{9}$	$I_1 I_4$
8	4	1	$\frac{(2+N)^2}{9}$	$\frac{4(6+N)}{27}$	$I_1 I_5$
9	4	1	$\frac{(2+N)(8+N)}{27}$	$\frac{2(2+N)(8+N)}{27}$	$-0.0266277+0.0012789y+0.000157474y^2 -0.000095736y^3+0.000031929y^4 -9.2602210-6y^5+O(y^6)$
10	4	2	$\frac{(2+N)(8+N)}{27}$	$\frac{8(4+N)}{27}$	$0.25-0.0601852y+0.0132661y^2-0.00292294y^3 +0.000651627y^4-0.000147057y^5+O(y^6)$
11	4	$\frac{1}{2}$	$\frac{(2+N)(8+N)}{27}$	$\frac{2(16+6N+N^2)}{27}$	$0.322467-0.0786798y+0.0175558y^2 -0.0039039y^3 +0.000\,876\,3y^4-0.000\,198\,793y^5+O(y^6)$

TABLE VII. Coefficients $\overline{e_{i,j}}$ and $\overline{a_{i,j}}$, cf. Eqs. (B4) and (B5).

i	j	$\overline{e_{i,j}}(8+N)^j/(2+N)^{(1-\delta_{j0})}$	$\overline{a_{i,j}}(N+8)^j$
1	0	$-\frac{1}{4}$	$-\frac{1}{4}$
	1	$\frac{1}{6}$	$\frac{1}{3}$
	2	0.0290678	$0.0581358-0.0195433N$
	3	$0.2941-0.0105012N$	$0.588201-0.158869N-0.044705N^2$
2	0	$\frac{1}{16}$	$\frac{1}{16}$
	1	$-\frac{1}{15}$	$-\frac{2}{15}$
	2	$0.0280008+0.0208333N$	$0.0560016+0.00585959N$
	3	$-0.046127+0.0223387N$	$-0.0922537+0.0828459N+0.0173899N^2$
3	0	$-\frac{1}{64}$	$-\frac{1}{64}$
	1	$\frac{71}{3360}$	$\frac{71}{1680}$
	2	$-0.0179798-0.0114583N$	$-0.0359598-0.00137167N$
	3	$0.00517395-0.00217669N+0.00231481N^2$	$0.0103479-0.0333737N-0.0056229N^2$
4	0	$\frac{1}{256}$	$\frac{1}{256}$
	1	$-\frac{31}{5040}$	$-\frac{31}{2520}$
	2	$0.00733893+0.0044494N$	$0.0146779+0.000299779N$
	3	$-0.000842908-0.00212265N+0.00162037N^2$	$-0.00168582+0.0117321N+0.00170808N^2$
5	0	$-\frac{1}{1024}$	$-\frac{1}{1024}$
	1	$\frac{3043}{1774080}$	$\frac{3043}{887}$
	2	$-0.00253604-0.00149678N$	$-0.00507208-0.0000641563N$
	3	$-0.000390898-0.0015352N-0.000747354N^2$	$0.000781794-0.0037964N-0.000501577N^2$

where we have explicitly written the mass dependence of the short-distance coefficient. Since renormalized correlation functions scale canonically, i.e.,

$$G_R^{(l)}(p,-p,0,\ldots,0)=m^{d-2l}f(p/m), \tag{A3}$$

we have

$$\tilde{C}(p;m)=m^{-2}\hat{C}(p/m). \tag{A4}$$

Renormalized correlation functions satisfy the Callan-Symanzik equation

$$\left[m\frac{\partial}{\partial m}+\beta(g)\frac{\partial}{\partial g}-l\,\eta_2(g)\right]G_R^{(l)}(p_1,\ldots,p_l)=m^2\sigma(g)G_R^{(l+1)}(0,p_1,\ldots,p_l). \tag{A5}$$

where $\sigma(g)$ is a RG function satisfying $\sigma(g^*)=2-\eta$ and $\eta_2(g)=\eta_t(g)-\eta_\phi(g)$. Applying the Callan-Symanzik equation to the relation (A2) we obtain, setting $g=g^*$,

$$\left[m\frac{\partial}{\partial m}-\eta_2(g^*)\right]\tilde{C}(p;m)=0, \tag{A6}$$

and therefore, using Eq. (A4), we have

$$\tilde{C}(p;m)\sim m^{-2}(p/m)^{-2-\eta_2}=m^{-2}(p/m)^{-1/\nu}. \tag{A7}$$

Now, using the above-reported results and $Z_t/Z_\phi\sim m^{\eta_t-\eta_\phi}\sim m^{1/\nu-2}$ for $g=g^*$, see Eq. (16), we obtain

$$\frac{\partial^2}{\partial t^2}G^{(2)}(p,-p)=G^{(4)}(0,0,p,-p)\sim m^{8-4/\nu}G_R^{(4)}(0,0,p,-p)$$
$$\approx m^{8-4/\nu}\tilde{C}(p;m)G_R^{(3)}(0,0,0)$$
$$\sim(p/m)^{-1/\nu}m^{d-4/\nu}\sim t^{-1-\alpha}p^{-1/\nu}. \tag{A8}$$

Integrating this equation twice with respect to t, we have

$$G^{(2)}(p,-p)=a(p)+b(p)t+ct^{1-\alpha}p^{-1/\nu}+o(t^{1-\alpha}), \tag{A9}$$

where $a(p)$ and $b(p)$ are unknown functions of p. Comparing this result with the scaling equations (32) and (33), we obtain finally Eq. (45).

2. The tensor correlation function

The calculation is analogous. The short-distance expansion of the product $T_{ij}(x)T_{ij}(y)$ is given by

TABLE VIII. Expansion coefficients x_1, x_2, and x_3 for e_i and a_i.

	x_1	x_2	x_3
e_1	$\frac{1}{12}$	$\frac{(2+N)(44+13N)}{12}$	$-\frac{7}{72}$
e_2	$-\frac{1}{120}$	$\frac{-40-270N-42N^2+N^3}{360}$	$\frac{7}{360}$
e_3	$\frac{1}{840}$	$\frac{-352+1176N+180N^2-5N^3}{10080}$	$-\frac{1}{240}$
e_4	$-\frac{1}{5040}$	$\frac{1808-3072N-477N^2+13N^3}{151200}$	$\frac{1}{1080}$
e_5	$\frac{1}{27720}$	$\frac{-3392+4208N+668N^2-17N^3}{1108800}$	$-\frac{1}{4752}$
a_1	$-\frac{1}{12}$	$\frac{22-N}{12}$	$\frac{7}{72}$
a_2	$\frac{1}{120}$	$\frac{-20+44N+3N^2}{720}$	$-\frac{7}{360}$
a_3	$-\frac{1}{840}$	$\frac{-88-128N-9N^2}{10080}$	$\frac{1}{240}$
a_4	$\frac{1}{5040}$	$\frac{904+778N+55N^2}{302400}$	$-\frac{1}{1080}$
a_5	$-\frac{1}{27720}$	$\frac{-2544-1768N-125N^2}{3326400}$	$\frac{1}{4752}$

$$T_{ij}(x+y/2)T_{ij}(x-y/2) = C_T(y)E(x) + (\text{less singular contributions}). \tag{A10}$$

Now, we consider the connected correlation function with l fields $E(x)$ and two fields $T_{ij}(x)$ with the indices summed over, $G_T^{(l)}(p_1,p_2;q_1,\ldots,q_l)$, and its renormalized counterpart

$$G_{T,R}^{(l)}(p_1,p_2;q_1,\ldots,q_l) = Z_T^2 Z_t^l Z_\phi^{-l-2} G_T^{(l)}(p_1,p_2;q_1,\ldots,q_l).$$

For $p \gg m$, we have

$$G_{T,R}^{(l)}(p,-p;0,\ldots,0) \approx \widetilde{C}_T(p;m) G_R^{(l+1)}(0,\ldots,0). \tag{A11}$$

The coefficient $\widetilde{C}_T(p;m)$ scales as in Eq. (A4) and satisfies the RG equation

$$\left[m\frac{\partial}{\partial m} - 2\eta_2' + \eta_2 \right] \widetilde{C}_T(p;m) = 0, \tag{A12}$$

where $\eta_2' = \eta_T - \eta_\phi$. Therefore,

$$\widetilde{C}_T(p;m) \sim m^{-2}(p/m)^{-2-2\eta_2'+\eta_2} = m^{-2}(p/m)^{-(1+\gamma_T-\alpha)/\nu}. \tag{A13}$$

As in the energy case, we consider the second derivative of $G_T^{(0)}(p,-p)$ with respect to t. For $p \gg m$, we have,

$$\begin{aligned} \frac{\partial^2}{\partial t^2} G_T^{(0)}(p,-p) &= G_T^{(2)}(p,-p;0,0) \\ &\sim m^{8-2/\nu-2\phi_T/\nu} G_{T,R}^{(2)}(p,-p;0,0) \\ &\approx m^{8-2/\nu-2\phi_T/\nu} \widetilde{C}(p;m) G_R^{(3)}(0,0,0) \\ &\sim p^{-(1+\gamma_T-\alpha)/\nu} t^{-1-\alpha}, \end{aligned} \tag{A14}$$

where we have used the fact that, for $g=g^*$, $Z_T/Z_\phi \sim m^{\eta_T-\eta_\phi} \sim m^{\phi_T/\nu-2}$, see Eqs. (16) and (20). Integrating this equation twice with respect to t and using the scaling equation (31), we obtain the large-momentum behavior (46).

APPENDIX B: PERTURBATIVE EXPANSION OF THE TWO-POINT FUNCTIONS $G_{E,T}$

In order to compute the structure factor of the bilinear fields, we determine the one-particle-irreducible diagrams with insertions of two operators E or T_{ij} and zero external legs. We use the susceptibility χ as inverse mass square, so that tadpole diagrams can be neglected. Also, subdiagrams

TABLE IX. Expansion coefficients x_4 and x_5 for e_i and a_i.

e_1	x_4	$\frac{-1184-348N-7N^2}{32}$
	x_5	$\frac{-(2+N)(-4112-2596N-466N^2+N^3)}{24}$
e_2	x_4	$\frac{4512+1420N+35N^2}{1280}$
	x_5	$\frac{(2+N)(-170624-78048N-8148N^2+509N^3)}{5760}$
e_3	x_4	$\frac{-2311264-726900N-17885N^2}{4587520}$
	x_5	$\frac{586167808+604936960N+160060792N^2+8862854N^3-1077019N^4+2048N^5}{61931520}$
e_4	x_4	$\frac{2370848+719452N+16023N^2}{27525120}$
	x_5	$\frac{-1006341632-1133004544N-290766168N^2-13609246N^3+2081479N^4-3072N^5}{619315200}$
e_5	x_4	$\frac{-2525643296-724481980N-13348335N^2}{155021475840}$
	x_5	$\frac{3084090980864+3778414828800N+961368439624N^2+41380542442N^3-6987518685N^4+2097152N^5}{10463949619200}$
a_1	x_4	$\frac{-1376+764N+301N^2+14N^3}{64}$
	x_5	$\frac{7552-2784N-5692N^2-1667N^3-100N^4}{96}$
a_2	x_4	$\frac{-(3104+12300N+3185N^2+140N^3)}{5120}$
	x_5	$\frac{-1087744-484736N+26236N^2+32387N^3+2316N^4}{23040}$
a_3	x_4	$\frac{1445632+1966400N+440020N^2+17885N^3}{4587520}$
	x_5	$\frac{568281088+262815488N-1452256N^2-13472924N^3-1114341N^4-9216N^5}{61931520}$
a_4	x_4	$\frac{-(33881888+34540972N+7018809N^2+256368N^3)}{440401920}$
	x_5	$\frac{-17032726784-7719736448N+90484812N^2+409316471N^3+36197264N^4+491520N^5}{9909043200}$
a_5	x_4	$\frac{5244438496+4565788340N+853347495N^2+26696670N^3}{310042951680}$
	x_5	$\frac{34179580035328+14923763131008N-513765484268N^2-895119755607N^3-81461592926N^4-1376256000N^5}{104639496192000}$

that correspond to diagrams of the two-point function $\langle\phi\phi\rangle$ are subtracted at zero momentum. The diagrams contributing up to four loops are drawn in Fig. 4. The structure factors of the bilinear fields can be expanded as

$$\mathcal{G}(\bar{g},y)=uG_{E,T}(u,q)=\sum_{j=1}(-1)^{l-1}u^l\chi^{l/2}S_jC_j^{E,T}I_j(q^2\chi), \tag{B1}$$

where the sum is over the graphs without tadpoles, l is the number of loops of the graph, S_j the graph symmetry factor, $C_j^{E,T}$ the group factor, and $I_j(q^2)$ the loop integral with unit mass. In Table VI, we report S_j and $C_j^{E,T}$.

We computed the coefficients $\bar{e}_i$ and $\bar{a}_i$ to four loops in the fixed-dimensions expansion. The expansion of the loop integrals $I_j(q^2)$ is reported in Table VI. In the calculation, we used the results of Refs. [61,62].

We also used the expression of the bare coupling u as a function of the renormalized coupling $\bar{g}$,

$$u = m\frac{48\pi\bar{g}}{(8+N)}\left[1+\bar{g}+\frac{27N^2+350N+1348}{27(8+N)^2}\bar{g}^2 + \frac{N^3+17.3632N^2+120.783N+315.831}{(8+N)^3}\bar{g}^3+O(\bar{g}^4)\right] \tag{B2}$$

and the relation between χ and m,

$$m^2\chi = Z_\phi(g) = 1-\frac{4(N+2)}{27(N+8)^2}\bar{g}^2 - 0.106\,993\frac{N+2}{(N+8)^2}\bar{g}^3 + O(\bar{g}^4). \tag{B3}$$

Writing

$$\bar{e}_i = \sum_{j=0}\bar{e}_{i,j}\bar{g}^j, \tag{B4}$$

$$\bar{a}_i = \sum_{j=0}\bar{a}_{i,j}\bar{g}^j, \tag{B5}$$

we computed the coefficients $\bar{e}_{i,j}$ and $\bar{a}_{i,j}$ up to $j=3$. They are reported in Table VII.

We computed the coefficients e_i and a_i in ϵ expansion to three loops, i.e., to order ϵ^3. The expansion of the integrals $I_4(y)$ and $I_5(y)$ was obtained by using the algebraic algorithm of Ref. [63].

We write

$$e_i = \frac{N-4}{N+8}x_1\epsilon + \frac{1}{(N+8)^3}x_2\epsilon^2 + \left[\frac{(N+2)(N-4)}{(N+8)^3}x_3\lambda + \frac{(N+2)}{(N+8)^4}x_4\zeta(3) + \frac{1}{(N+8)^5}x_5\right]\epsilon^3 + O(\epsilon^4), \tag{B6}$$

$$a_i = \frac{N+4}{N+8}x_1\epsilon + \frac{N+4}{(N+8)^3}x_2\epsilon^2 + \left[\frac{(N+2)(N+4)}{(N+8)^3}x_3\lambda + \frac{1}{(N+8)^4}x_4\zeta(3) + \frac{1}{(N+8)^5}x_5\right]\epsilon^3 + O(\epsilon^4), \tag{B7}$$

where $\lambda = 1.171\,953\,619\,344\,729\,445$. The coefficients x_i are reported in Tables VIII and IX. Note that [11] to order ϵ^2, $e_1 \approx -\alpha/(6\gamma)$ and $a_1 \approx -\gamma_T/(6\gamma)$. These relations do not hold at order ϵ^3.

[1] A. Pelissetto and E. Vicari, e-print cond-mat/0012164.
[2] M. E. Fisher and P. Pfeuty, Phys. Rev. B **6**, 1889 (1972).
[3] F. J. Wegner, Phys. Rev. B **6**, 1891 (1972).
[4] M. E. Fisher and D. Nelson, Phys. Rev. Lett. **32**, 1350 (1974).
[5] A. Aharony, in *Phase Transitions and Critical Phenomena*, edited by C. Domb and J. L. Lebowitz (Academic Press, New York, 1976), Vol. 6, p. 357.
[6] P. Pfeuty, D. Jasnow, and M. E. Fisher, Phys. Rev. B **10**, 2088 (1974).
[7] M. E. Fisher, Phys. Rev. Lett. **34**, 1634 (1975).
[8] J. M. Kosterlitz, D. R. Nelson, and M. E. Fisher, Phys. Rev. Lett. **33**, 813 (1974); Phys. Rev. B **13**, 412 (1976).
[9] S.-C. Zhang, Science **275**, 1089 (1997).
[10] S. Murakami and N. Nagaosa, J. Phys. Soc. Jpn. **69**, 2395 (2000).
[11] R. R. Netz and A. Aharony, Phys. Rev. E **55**, 2267 (1997).
[12] For a general review, see J. D. Litster and R. J. Birgeneau, Phys. Today **35**(5), 261 (1982).
[13] E. Fawcett, Rev. Mod. Phys. **60**, 1 (1988).
[14] A. Aharony, R. J. Birgeneau, J. D. Brock, and J. D. Litster, Phys. Rev. Lett. **57**, 1012 (1986).
[15] J. D. Brock, D. Y. Noh, B. R. McClain, J. D. Litster, R. J. Birgeneau, A. Aharony, P. M. Horn, and J. C. Liang, Z. Phys. B: Condens. Matter **74**, 197 (1989).
[16] C. W. Garland, G. Nounesis, M. J. Young, and R. J. Birgeneau, Phys. Rev. E **47**, 1918 (1993).
[17] L. Wu, M. J. Young, Y. Shao, C. W. Garland, R. J. Birgeneau, and G. Heppke, Phys. Rev. Lett. **72**, 376 (1994).
[18] A. Aharony, R. J. Birgeneau, C. W. Garland, Y.-J. Kim, V. V. Lebedev, R. R. Netz, and M. J. Young, Phys. Rev. Lett. **74**, 5064 (1995).
[19] A. Aharony, Phys. Rev. B **44**, 423 (1991).
[20] J. F. Fernández, Phys. Rev. B **38**, 6901 (1988).
[21] Y. Yamazaki, Phys. Lett. **49A**, 215 (1974).
[22] X. Hu, Phys. Rev. Lett. **87**, 057 004 (2001).
[23] G. Parisi, J. Stat. Phys. **23**, 49 (1980).
[24] A. J. Bray, Phys. Rev. B **14**, 1248 (1976).
[25] G. A. Baker, Jr., B. G. Nickel, M. S. Green, and D. I. Meiron, Phys. Rev. Lett. **36**, 1351 (1977); G. A. Baker, Jr., B. G. Nickel, and D. I. Meiron, Phys. Rev. B **17**, 1365 (1978).
[26] S. A. Antonenko and A. I. Sokolov, Phys. Rev. E **51**, 1894 (1995).
[27] D. B. Murray and B. G. Nickel, Revised estimates for critical exponents for the continuum *n*-vector model in 3 dimensions, Guelph University Report, 1991 (unpublished).
[28] B. G. Nickel, D. I. Meiron, and G. A. Baker, Jr., Compilation of 2-pt and 4-pt graphs for continuum spin models, Guelph University Report, 1977 (unpublished).
[29] J. C. Le Guillou and J. Zinn-Justin, Phys. Rev. Lett. **39**, 95 (1977); Phys. Rev. B **21**, 3976 (1980).
[30] J. Zinn-Justin, *Quantum Field Theory and Critical Phenomena*, 3rd ed. (Clarendon Press, Oxford, 1996).
[31] J. M. Carmona, A. Pelissetto, and E. Vicari, Phys. Rev. B **61**, 15 136 (2000).
[32] In the analyses we used the following estimates of $\bar{g}^*$: $\bar{g}^* = 1.405(2)$ for $N=1$ (from Ref. [1]), $\bar{g}^* = 1.402(4)$ for $N=2$ (from Ref. [33]), $\bar{g}^* = 1.395(7)$ for $N=3$ (from Ref. [64]), $\bar{g}^* = 1.385(15)$, 1.360(15), 1.310(15), 1.205(15) for

$N=4,5,8,16$ respectively (from Refs. [63,65,66]). Other numerical estimates can be found in Ref. [1].

[33] M. Campostrini, M. Hasenbusch, A. Pelissetto, P. Rossi, and E. Vicari, Phys. Rev. B **63**, 214 503 (2001).

[34] A. Pelissetto and E. Vicari, Nucl. Phys. B **519**, 626 (1998).

[35] P. Calabrese, M. Caselle, A. Celi, A. Pelissetto, and E. Vicari, J. Phys. A **33**, 8155 (2000).

[36] M. Caselle, A. Pelissetto, and E. Vicari, in *Fluctuating Paths and Fields*, edited by W. Janke, A. Pelster, H.-J. Schmidt, and M. Bachmann (World Scientific, Singapore, 2001); e-print hep-th/0010228.

[37] For the exponent ν we have taken the following numerical results: $\nu=0.630\,02(23)$ for $N=1$ (Ref. [44]), $\nu=0.671\,55(27)$ for $N=2$ (Ref. [33]), $\nu=0.7112(5)$ for $N=3$ (Ref. [64]), $\nu=0.749(2)$ for $N=4$ (Ref. [67]), $\nu=0.766$, 0.830, 0.911 for $N=5,8,16$ (Ref. [26]). Other numerical estimates can be found in Ref. [1].

[38] S. Hikami and R. Abe, Prog. Theor. Phys. **52**, 369 (1974); R. Oppermann, Phys. Lett. **47A**, 383 (1974).

[39] V. Privman, P. C. Hohenberg, and A. Aharony, in *Phase Transitions and Critical Phenomena*, edited by C. Domb and J. L. Lebowitz (Academic Press, New York, 1991), Vol. 14.

[40] H. Rohrer and Ch. Gerber, Phys. Rev. Lett. **38**, 909 (1977).

[41] A. R. King and H. Rohrer, Phys. Rev. B **19**, 5864 (1979).

[42] M. E. Fisher and R. J. Burford, Phys. Rev. **156**, 583 (1967).

[43] M. E. Fisher and A. Aharony, Phys. Rev. Lett. **31**, 1238 (1973); Phys. Rev. B **10**, 2818 (1974).

[44] M. Campostrini, A. Pelissetto, P. Rossi, and E. Vicari, Phys. Rev. E **60**, 3526 (1999); e-print cond-mat/0201180.

[45] M. Hasenbusch, J. Phys. A **32**, 4851 (1999).

[46] M. Campostrini, A. Pelissetto, P. Rossi, and E. Vicari, Phys. Rev. E **57**, 184 (1998).

[47] M. E. Fisher and J. S. Langer, Phys. Rev. Lett. **20**, 665 (1968).

[48] E. Brézin, J. C. Le Guillou, and J. Zinn-Justin, in *Phase Transitions and Critical Phenomena*, edited by C. Domb and J. Lebowitz (Academic Press, New York, 1976), Vol. 6, p. 125.

[49] J. C. Le Guillou and J. Zinn-Justin, J. Phys. (France) **48**, 19 (1987).

[50] A. Pelissetto and E. Vicari, Nucl. Phys. B **522**, 605 (1998).

[51] S. Caracciolo, R. G. Edwards, T. Mendes, A. Pelissetto, and A. D. Sokal, Nucl. Phys. B (Proc. Suppl.) **47**, 763 (1996).

[52] T. Mendes, A. Pelissetto, and A. D. Sokal, Nucl. Phys. B **477**, 203 (1996).

[53] A. Cucchieri, T. Mendes, A. Pelissetto, and A. D. Sokal, J. Stat. Phys. **86**, 581 (1997).

[54] R. R. Netz and I. H. Gersonde, J. Phys. I **7**, 827 (1997).

[55] The same singular behavior for $N\rightarrow4$ is present in the ϵ expansion of the coefficients A_i of the large-momentum expansion of the fundamental two-point function, cf. Eq. (44). Indeed, one finds [43] $A_1=1+O(\epsilon)$, $A_2=(2+N)/(4-N)+O(\epsilon)$, and $A_3=-6/(4-N)+O(\epsilon)$.

[56] A. Aharony, e-print cond-mat/0107585.

[57] R. M. Fleming, D. E. Moncton, J. D. Axe, and G. S. Brown, Phys. Rev. B **30**, 1877 (1984).

[58] S. Girault, A. H. Moudden, and J. P. Pouget, Phys. Rev. B **39**, 4430 (1989).

[59] P. Calabrese, A. Pelissetto, and E. Vicari, e-print cond-mat/0111512.

[60] E. Brézin, D. J. Amit, and J. Zinn-Justin, Phys. Rev. Lett. **32**, 151 (1974).

[61] B. G. Nickel, J. Math. Phys. **19**, 542 (1977).

[62] A. K. Rajantie, Nucl. Phys. B **480**, 729 (1996); **513**, 761(E) (1998).

[63] A. Pelissetto and E. Vicari, Nucl. Phys. B **575**, 579 (2000).

[64] M. Campostrini, M. Hasenbusch, A. Pelissetto, P. Rossi, and E. Vicari, e-print cond-mat/0110336, Phys. Rev. B (to be published).

[65] R. Guida and J. Zinn-Justin, J. Phys. A **31**, 8103 (1998).

[66] P. Butera and M. Comi, Phys. Rev. B **58**, 11 552 (1998).

[67] M. Hasenbusch, J. Phys. A **34**, 8221 (2001).